

Thermal behavior and other properties of Pr(III), Sm(III), Eu(III), Gd(III), Tb(III) complexes with 4,4'-bipyridine and trichloroacetates

A. Czyłkowska · D. Czakis-Sulikowska ·
A. Kaczmarek · M. Markiewicz

Received: 17 October 2010 / Accepted: 7 March 2011 / Published online: 1 April 2011
© The Author(s) 2011. This article is published with open access at Springerlink.com

Abstract A novel mixed-ligand complexes with empirical formulae: $\text{Ln}(4\text{-bpy})_{1.5}(\text{CCl}_3\text{COO})_3 \cdot n\text{H}_2\text{O}$ (where Ln(III) = Pr, Sm, Eu, Gd, Tb; $n = 1$ for Pr, Sm, Eu and $n = 3$ for Gd, Tb; 4-bpy = 4,4'-bipyridine) were prepared and characterized by chemical, elemental analysis and IR spectroscopy. Conductivity studies (in methanol, dimethylformamide and dimethylsulfoxide) were also described. All complexes are crystalline. The way of metal–ligand coordination was discussed. The thermal properties of complexes in the solid state were studied under non-isothermal conditions in air atmosphere. During heating the complexes decompose via intermediate products to the oxides: Pr_6O_{11} , Ln_2O_3 (for Sm, Eu, Gd) and Tb_4O_7 . TG-MS system was used to analyze principal volatile thermal decomposition and fragmentation products evolved during pyrolysis of Pr(III) and Sm(III) compounds in air.

Keywords Lanthanide complexes · 4,4'-bipyridine · Trichloroacetates · Thermal decomposition

Introduction

This work is a continuation of our previous studies on synthesis, properties, and thermal decomposition of metal complexes with bipyridine isomers and carboxylates [1–7]. Lanthanide compounds are curious for many research workers in last years because of their variety applications

[8–13]. Halogenoacetates complexes show varied types of coordination, therefore they are interesting ligands.

Authors [14–18] isolated compounds type: $\text{Ln}(\text{CCl}_2\text{HCOO})_3 \cdot 2\text{H}_2\text{O}$ (where Ln(III) = Pr, Er), $\text{Ln}(\text{CCl}_3\text{COO})_3 \cdot 2\text{H}_2\text{O}$ (where Ln(III) = Pr, Nd, Eu, Dy, Yb), $[\text{Nd}(\text{CCl}_2\text{HCOO})_6(\text{H}_2\text{O})_3]_n \cdot m\text{H}_2\text{O}$ and $\text{Nd}_x\text{Ln}_{1-x}(\text{CCl}_3\text{COO})_3 \cdot 2\text{H}_2\text{O}$. In 2003 year $[\text{Tb}_2(\text{CH}_3\text{COO})_6(\text{H}_2\text{O})_4] \cdot 4\text{H}_2\text{O}$ and $[\text{Tb}_2(\text{CF}_3\text{COO})_6(\text{H}_2\text{O})_6]$ complexes were produced [19]. Rohde and Urland [20] obtained monocystals $\text{Ln}(\text{CClF}_2\text{COO})_3 \cdot 3\text{H}_2\text{O}$ (where Ln(III) = Gd, Dy, Ho and Er). There is report about crystal structure of neodymium(III) compounds with monochloroacetate [21]. Imai et al. [22] synthesized and characterized $[\text{Ln}(\text{CCl}_2\text{HCOO})_3(\text{H}_2\text{O})_5]_n$ (where Ln(III) = La, Pr, Nd, Eu) and their properties were measured.

There are scant information about lanthanide complexes with bipyridine isomers and halogenoacetates. Authors [23, 24] synthesized and determined crystal structure of compounds type: $[\text{Ln}(\text{CCl}_2\text{HCOO})_3(2\text{-bpy})]_n$ (where Ln(III) = Nd, Pr; 2-bpy = 2,2'-bipyridine). Single crystals of $[\text{Gd}_2(\text{CClF}_2\text{COO})_6(\text{H}_2\text{O})_2(2\text{-bpy})_2]_2 \cdot \text{C}_2\text{H}_5\text{OH}$ have been obtained [25]. Crystal structure and magnetic properties of the gadolinium complexes type: $\text{Gd}_2(\text{CClH}_2\text{COO})_6(2\text{-bpy})_2$ [26] and $\text{Gd}_2(\text{CCl}_3\text{COO})_6(2\text{-bpy})_2(\text{H}_2\text{O})_2 \cdot 4(2\text{-bpy})$ [27] were measured. Authors [27] described also compounds $\text{Ln}(\text{CCl}_3\text{COO})_3(2\text{-bpy})_2$ (Ln(III) = Pr, Nd). Spacu and Antonescu [28] reported thermal stability and some properties of complexes $[\text{LnA}_3(\text{N-donors})] \cdot n\text{H}_2\text{O}$ (where Ln(III) = La → Eu (expect Pm), Dy and Er; A = chloroacetates; N-donors = 1,10-phenantroline, 2,2'-bipyridine and 4,7-diphenyl-1,10-phenantroline). Hart and Laming [29] described synthesis of complexes $\text{Ln}(2\text{-bpy})\text{X}_3 \cdot n\text{H}_2\text{O}$ where Ln(III) = La, Pr, Ce, Nd, Sm, Eu, Dy, Er; X = chloroacetates. Kokonov et al. [30] characterized thermal studies of compounds neodymium and erbium with 2-bpy and dibromoacetates.

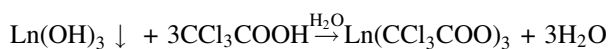
A. Czyłkowska (✉) · D. Czakis-Sulikowska · A. Kaczmarek ·
M. Markiewicz
Institute of General and Ecological Chemistry, Technical
University of Lodz, Lodz, Poland
e-mail: agnieszka.czyłkowska@p.lodz.pl

Owing to two nitrogen donor atoms 4,4'-bipyridine is used as a potential ligand. This isomer creating polymeric species [31–34]. In combination with carboxylate groups 4-bpy makes up interesting structures [35–39]. Our studies presented here complete series of lanthanides metal complexes with 4,4'-bipyridine and halogenoacetates [35, 40–44].

Experimental

Materials

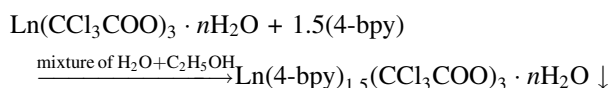
All the chemicals and solvents used were of analytical grade. Trichloroacetic acid was obtained from Reanal–Budapest, methanol (MeOH, anhydrous) from Scan–Lab, $\text{SmCl}_3 \cdot 6\text{H}_2\text{O}$ from Aldrich, Tb_4O_7 Koch Light Laboratory England and Pr_6O_{11} Rare Earth Products Limited. 4,4'-Bipyridine, Eu_2O_3 , Gd_2O_3 and other products were obtained from POCh–Gliwice. Solutions of lanthanide(III) trichloroacetates as hydrated products were prepared by dissolving freshly precipitated hydroxides in 2 mol L^{-1} CCl_3COOH in stoichiometric quantities (pH 5) according to the reaction:



where Ln(III) = Pr(III), Sm(III), Eu(III), Gd(III), Tb(III).

Synthesis and analysis

The contents of Ln(III) ions in obtained solutions of trichloroacetates were complexometrically (EDTA) determined. The mixed-ligand complexes were prepared by mixing 10 mmol of 4-bpy in 96% v/v ethanol (31.25 mL) with the freshly obtained solution of 5 mmol metal trichloroacetates in 8.75 mL of water at room temperature. The equation for synthesis of complexes:



During several days the compounds crystallized. The obtained complexes were filtered off; washed with 40% v/v ethanol and then with EtOH and Et_2O mixture (1:1) and air dried at room temperature. The contents of N, H, and C in prepared complexes were determined by a Carbo-Erba analyzer with V_2O_5 as an oxidizing agent; metals(III) in mineralized samples complexometrically.

Methods and instruments

IR spectra were recorded with a NICOLETT 6700 Spectrometer ($4000\text{--}400 \text{ cm}^{-1}$ with accuracy of recording 1 cm^{-1}) using KBr pellets. Molar conductance was

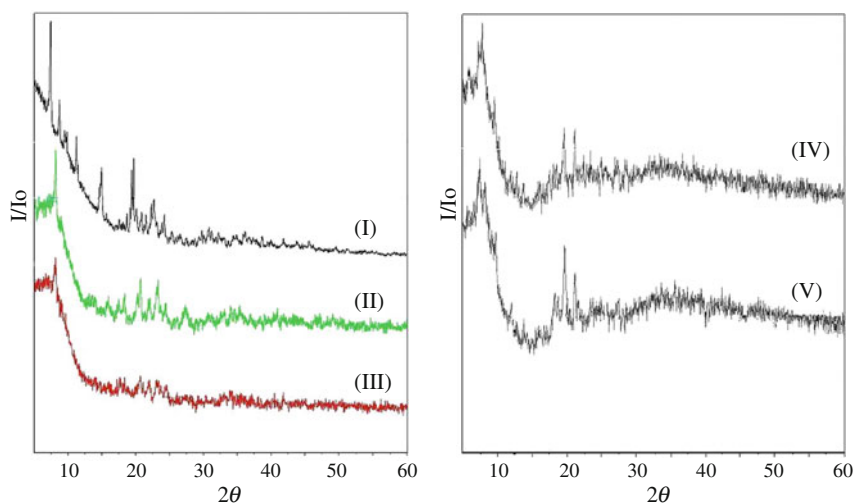
measured on a conductivity meter of the OK-102/1 type equipped with an OK-902 electrode at $298 \pm 0.5 \text{ K}$, using $1 \times 10^{-3} \text{ mol L}^{-1}$ solutions of complexes in methanol (MeOH), dimethylsulfoxide (DMSO) and dimethylformamide (DMF). The thermal properties of complexes were studied by TG, DTG and DTA techniques; TG, DTG and DTA curves were recorded on derivatograph type Q-1500, samples of 100 mg, $\alpha\text{-Al}_2\text{O}_3$ served as reference material in air static atmosphere. From TG, DTA and DTG curves the solid intermediate products decomposition were determined and were confirmed by the IR spectra of sinters. In sinters (prepared during heating of complexes up to temperatures defined from TG curves) the vibration modes of 4-bpy and trichloroacetates were analyzed as well as the presence of anions Cl^- was also stated. The TG-MS system, consisted of a TG/DTA-SETSIS-16/18 coupled to a mass spectrometer (QMS-422; ThermoStar from Balzers Instruments, an ion source of ca 423 K by using 70 eV electron impact ionization and flow rate 1 L/h), used to monitored principal volatile species produced during pyrolysis of the Pr(III) and Sm(III) complexes (with samples of mass 4.64 and 4.82 mg, respectively) in dynamic air atmosphere. The m/z values are given based on ^1H , ^{12}C , ^{14}N , ^{16}O , and ^{35}Cl (additionally ^{13}C and ^{18}O in case of CO_2). All thermal investigations were carried out in the range of temperature 293–1273 K at a heating rate of 10 K min^{-1} . For all complexes and final solid decomposition products, X-ray diffractograms (D-5000 diffractometer, Ni-filtered CuK_α radiation) were done in the range of 2θ angles 2–80°. Obtained results were analyzed using the Powder Diffraction File [45].

Results and discussion

The analytical data are shown in Table 1. These results establish the stoichiometry of these compounds with the general empirical formulae: $\text{Ln}(4\text{-bpy})_{1.5}(\text{CCl}_3\text{COO})_3 \cdot \text{H}_2\text{O}$ (where Ln(III) = Pr, Sm, Eu) and $\text{Ln}(4\text{-bpy})_{1.5}(\text{CCl}_3\text{COO})_3 \cdot 3\text{H}_2\text{O}$ (Ln(III) = Gd, Tb). The observed molar conductivities values in MeOH, DMSO, and DMF are given also in Table 1. Conductivity measurements suggested that in all solutions of obtained compounds have behavior non-electrolytes (they dissociate in limited degree in these solutions) [46]. This indicates that trichloroacetate anions are located in the coordination sphere. All complexes are stable in air at room temperature for ca 5 months. The X-ray diffraction powder patterns (Fig. 1) show that all the compounds have crystalline structure and the crystallinity of these complexes follows the order: $\text{Pr} > \text{Sm} > \text{Gd} \approx \text{Tb} > \text{Eu}$. Difference in the crystallinity of these compounds probably depends on the velocity of the evaporation which

Table 1 Analytical data and molar conductivity in MeOH, DMF, and DMSO for the $\text{Ln}(4\text{-bpy})_{1.5}(\text{CCl}_3\text{COO})_3 \cdot n\text{H}_2\text{O}$

Compound (color)	Analysis: found (calculated)/%				$\Lambda_{\text{M}}(\Omega^{-1} \text{ cm}^2 \text{ mol}^{-1}); c = 1 \times 10^{-3} \text{ mol L}^{-1}$		
	Ln	C	N	H	MeOH	DMF	DMSO
(I) $\text{Pr}(4\text{-bpy})_{1.5}(\text{CCl}_3\text{COO})_3 \cdot \text{H}_2\text{O}$ (light green)	16.36 (16.01)	28.73 (28.65)	5.05 (4.77)	1.57 (1.60)	58.6	19.8	14.7
(II) $\text{Sm}(4\text{-bpy})_{1.5}(\text{CCl}_3\text{COO})_3 \cdot \text{H}_2\text{O}$ (light yellow)	17.72 (16.90)	28.41 (28.35)	4.72 (4.72)	1.55 (1.59)	56.6	20.2	9.7
(III) $\text{Eu}(4\text{-bpy})_{1.5}(\text{CCl}_3\text{COO})_3 \cdot \text{H}_2\text{O}$ (white)	16.60 (17.05)	28.39 (28.30)	4.98 (4.71)	1.52 (1.58)	55.1	17.4	7.3
(IV) $\text{Gd}(4\text{-bpy})_{1.5}(\text{CCl}_3\text{COO})_3 \cdot 3\text{H}_2\text{O}$ (white)	17.18 (16.89)	27.11 (27.04)	4.39 (4.51)	1.91 (1.95)	59.6	20.4	27.7
(V) $\text{Tb}(4\text{-bpy})_{1.5}(\text{CCl}_3\text{COO})_3 \cdot 3\text{H}_2\text{O}$ (white)	17.59 (17.01)	27.08 (26.99)	4.91 (4.50)	1.89 (1.94)	55.0	18.0	14.1

Fig. 1 X-ray diffraction patterns for complexes $\text{Ln}(4\text{-bpy})_{1.5}(\text{CCl}_3\text{COO})_3 \cdot \text{H}_2\text{O}$ (I–III) and $\text{Ln}(4\text{-bpy})_{1.5}(\text{CCl}_3\text{COO})_3 \cdot 3\text{H}_2\text{O}$ for (IV) and (V)

was not controlled. They are isostructural in the groups: Pr, Sm, Eu and Gd, Tb. Some complexes in solid state show fluorescence at room temperature: Eu (intensive pink) and Tb (light green). This fluorescence was observed in the light of an LS/58 quartz lamp at room temperature.

IR spectra

IR spectra of the all obtained complexes exhibit several absorption bands characteristic for 4-bpy and $-\text{COO}$ groups. The fundamental vibration modes of 4-bpy and $-\text{COO}$ groups for complexes are reported in Table 2. The IR spectrum of free 4,4'-bipyridine undergoes a modification when coordination with a lanthanide. The most characteristic ring vibration modes $\nu(\text{CC})$, $\nu(\text{CN})$, $\nu(\text{CC}_{\text{ip}})-A_1$ symmetry and $\nu(\text{CC})$, $\nu(\text{CN})-B_1$ symmetry appear at 1588 and 1530 cm^{-1} in the free ligand [47]. In the IR spectra of complexes they are observed at 1602–1600 and 1534–1533 cm^{-1} , respectively. The ring deformation modes are between 1002 and 1000 cm^{-1} shifted to higher

frequencies in comparison with free 4-bpy (988 cm^{-1}). The bathochromic shifts of principal absorption bands suggest that 4-bpy is coordinated to Ln(III) ions [47].

The IR spectra of $\text{Ln}(4\text{-bpy})_{1.5}(\text{CCl}_3\text{COO})_3 \cdot \text{H}_2\text{O}$ (Ln(III) = Pr, Sm, Eu) show asymmetric $\nu_{\text{as}}(\text{COO})$ and symmetric $\nu_{\text{s}}(\text{COO})$ vibration of $-\text{COO}$ groups in the range 1671–1646 and 1371–1367 cm^{-1} , respectively. On the grounds of spectroscopic criteria [44, 48–51] it can be stated, that in case of Pr(III), Sm(III) and Eu(III) complexes carboxylate groups are bonded as bidentate chelating ligand (the values of $\Delta\nu = \nu_{\text{as}} - \nu_{\text{s}}$ of these complexes are smaller than for sodium salt $\Delta\nu_{\text{Na}} = 324$).

In the case of complexes $\text{Ln}(4\text{-bpy})_{1.5}(\text{CCl}_3\text{COO})_3 \cdot 3\text{H}_2\text{O}$ (Ln(III) = Gd, Tb) the ν_{s} is splitted into doublet. Therefore, we may suppose that non-completely equivalent bands (probably chelating and bridging or tridentate chelating-bridging [52]) between Ln(III) (Gd, Tb) and carboxylate groups of trichloroacetate ligands are formed. The different types of bonds between lanthanide(III) and carboxylate ligands within one molecule in reported in the literature [19, 21, 32, 33]. A broad band in the water

Table 2 Principal IR bands (cm^{-1}) for 4-bpy and COO group in obtained complexes

Assignment of bands	4-bpy [47]	CCl_3COONa [48]	Complexes of Ln(III)				
			Pr	Sm	Eu	Gd	Tb
Coordinated 4,4'-bipyridine modes							
$\nu(\text{CC}, \text{CN}, \text{C}_{i,r}) A_1$	1588	–	1602	1600	1601	1600	1601
$\nu(\text{CC}, \text{CN}) B_1$	1530	–	1533	1533	1533	1533	1534
Ring deformation	988	–	1001	1000	1001	1002	1002
Carboxylate group modes							
$\nu_{\text{as}}(\text{COO})$	–	1677	1646	1653	1671	1674	1670
$\nu_{\text{s}}(\text{COO})$	–	1353	1371	1367	1367	1367	1372
						1348	1344
$\Delta\nu = \nu_{\text{as}}(\text{COO}) - \nu_{\text{s}}(\text{COO})$	–	324	275	286	304	307	298
						326	326

Table 3 Thermal decomposition data of obtained complexes in air; mass sample 100 mg

No.	Complex	Range of decomposition/K	DTA peaks/K	Mass loss/%		Intermediate and residue solid products
				Found	Calc.	
(I)	$\text{Pr}(4\text{-bpy})_{1.5}(\text{CCl}_3\text{COO})_3 \cdot \text{H}_2\text{O}$	333–391	388 endo	2.5	2.05	$\text{Pr}(4\text{-bpy})_{1.5}(\text{CCl}_3\text{COO})_3$
		391–513	503 exo	43.0	43.25	$\text{Pr}(4\text{-bpy})_{1.5}\text{Cl}_3$
		513–1053	978 exo	35.0	35.36	Pr_6O_{11}
(II)	$\text{Sm}(4\text{-bpy})_{1.5}(\text{CCl}_3\text{COO})_3 \cdot \text{H}_2\text{O}$	333–418	378 endo	13.0	12.72	$\text{Sm}(4\text{-bpy})_{1.5}(\text{CCl}_3\text{COO})_{2.25}\text{Cl}_{0.75}$
		418–523	453 exo	33.0	32.10	$\text{Sm}(4\text{-bpy})_{1.5}\text{Cl}_3$
		523–668	593 endo	8.5	–	^a
		668–1053	723, 783, 1023 exo	24.0	23.72	SmOCl
		1053–1213	1083 endo	2.5	3.08	Sm_2O_3
(III)	$\text{Eu}(4\text{-bpy})_{1.5}(\text{CCl}_3\text{COO})_3 \cdot \text{H}_2\text{O}$	333–408	373 endo	19.5	19.82	$\text{Eu}(4\text{-bpy})_{1.5}(\text{CCl}_3\text{COO})_{1.75}\text{Cl}_{1.25}$
		408–468	463 exo	26.0	24.92	$\text{Eu}(4\text{-bpy})_{1.5}\text{Cl}_3$
		468–718	653 endo	17.0	–	^a
		718–893	703, 838 exo	15.0	14.92	EuOCl
		>893		2.5	3.08	Eu_2O_3
(IV)	$\text{Gd}(4\text{-bpy})_{1.5}(\text{CCl}_3\text{COO})_3 \cdot 3\text{H}_2\text{O}$	333–413	368 endo	21.0	21.0	$\text{Gd}(4\text{-bpy})_{1.5}(\text{CCl}_3\text{COO})_2\text{Cl}$
		413–483	463 exo	27.0	27.0	$\text{Gd}(4\text{-bpy})_{1.5}\text{Cl}_3$
		483–763	733 exo	13.0	–	^a
		763–1043	813, 1023 exo	17.0	17.0	GdOCl
		>1123		3.0	3.0	Gd_2O_3
(V)	$\text{Tb}(4\text{-bpy})_{1.5}(\text{CCl}_3\text{COO})_3 \cdot 3\text{H}_2\text{O}$	333–403	353 endo	20.0	19.37	$\text{Tb}(4\text{-bpy})_{1.5}(\text{CCl}_3\text{COO})_2\text{Cl}$
		403–573	453 exo	39.0	39.70	$\text{Tb}(4\text{-bpy})_{0.75}\text{Cl}_3$
		573–753	723 exo	5.0	–	^a
		753–988	808, 953 exo	14.0	14.24	TbOCl
		>988		3.0	2.51	Tb_4O_7

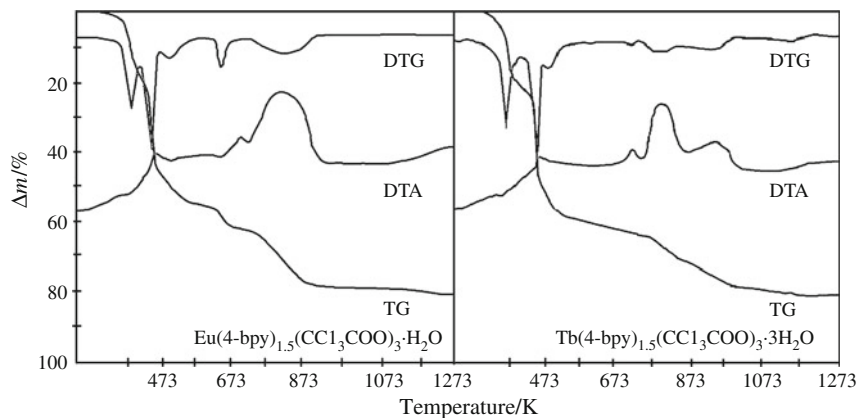
^a Probably via $\text{Ln}(4\text{-bpy})_{1.5-m}\text{Cl}_3$

stretching region ($3550\text{--}3200\text{ cm}^{-1}$) and only shoulder in the water bending region (ca $1630\text{--}1600\text{ cm}^{-1}$) are observed for all complexes.

In addition, in obtained compounds there are bands in the ranges: $837\text{--}683\text{ cm}^{-1}$ for Pr(III), $839\text{--}681\text{ cm}^{-1}$ for Sm(III), $838\text{--}680\text{ cm}^{-1}$ for Eu(III), $837\text{--}680\text{ cm}^{-1}$ for

Gd(III) and $838\text{--}681\text{ cm}^{-1}$ for Tb(III). These absorptions are associated with several vibrations: $\nu(\text{CCl})$ ($800\text{--}550\text{ cm}^{-1}$), $\nu_{\text{as}}(\text{CCl}_3)$ ($849, 833\text{ cm}^{-1}$), $\nu_{\text{s}}(\text{CCl}_3)$ ($746, 685\text{ cm}^{-1}$), $\gamma(\text{CH})$ 4-sub pyridine ($810, 745, 733, 672\text{ cm}^{-1}$) [47–49]. Probably, the medium absorption band at ca 440 cm^{-1} is result of overlap the vibrations of $\nu(\text{Ln}\text{--}\text{O})$ and $\rho_{\text{r}}(\text{COO})$

Fig. 2 Thermoanalytical curves of complexes Eu(III) and Tb(III) in air; mass sample 100 mg



[49, 53, 54]. Thus, the interpretation of IR spectra in these regions is difficult to discuss.

Thermal decomposition

Thermal decomposition of analyzed complexes in air is a multistage process. The solid intermediate products of

pyrolysis were determined from TG and DTG curves. The thermal decomposition data are collected in Table 3. Figure 2 presents, as an example, the thermoanalytical curves of $\text{Eu}(4\text{-bpy})_{1.5}(\text{CCl}_3\text{COO})_3 \cdot \text{H}_2\text{O}$ and $\text{Tb}(4\text{-bpy})_{1.5}(\text{CCl}_3\text{COO})_3 \cdot 3\text{H}_2\text{O}$. All the compounds are stable to 333 K. DTA curves present several endo- and exothermic peaks. The very strong and broad exothermic effects correspond to

Fig. 3 Some profiles of ion current detected in the mass spectrometer versus time for complexes Pr(4-bpy)_{1.5}(CCl₃COO)₃·H₂O (mass sample 4.64 mg) (I) and Sm(4-bpy)_{1.5}(CCl₃COO)₃·H₂O (mass sample 4.82 mg) (II), in air, for *m/z* values; heating rate 10 K min⁻¹

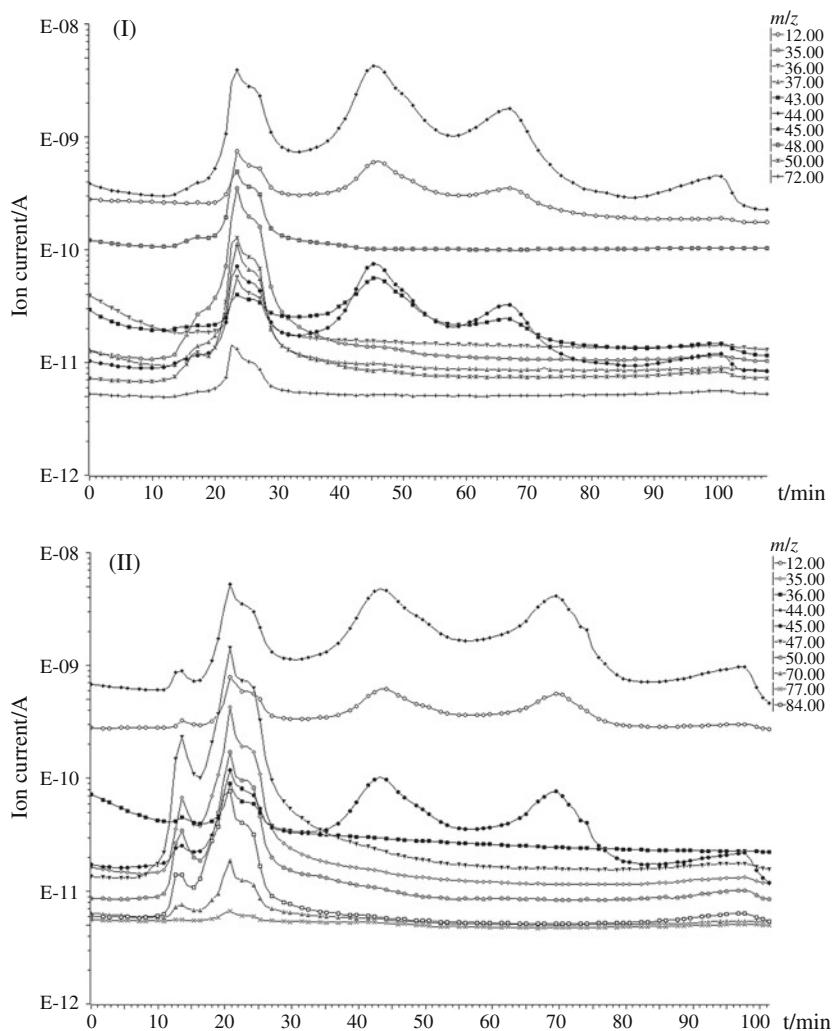
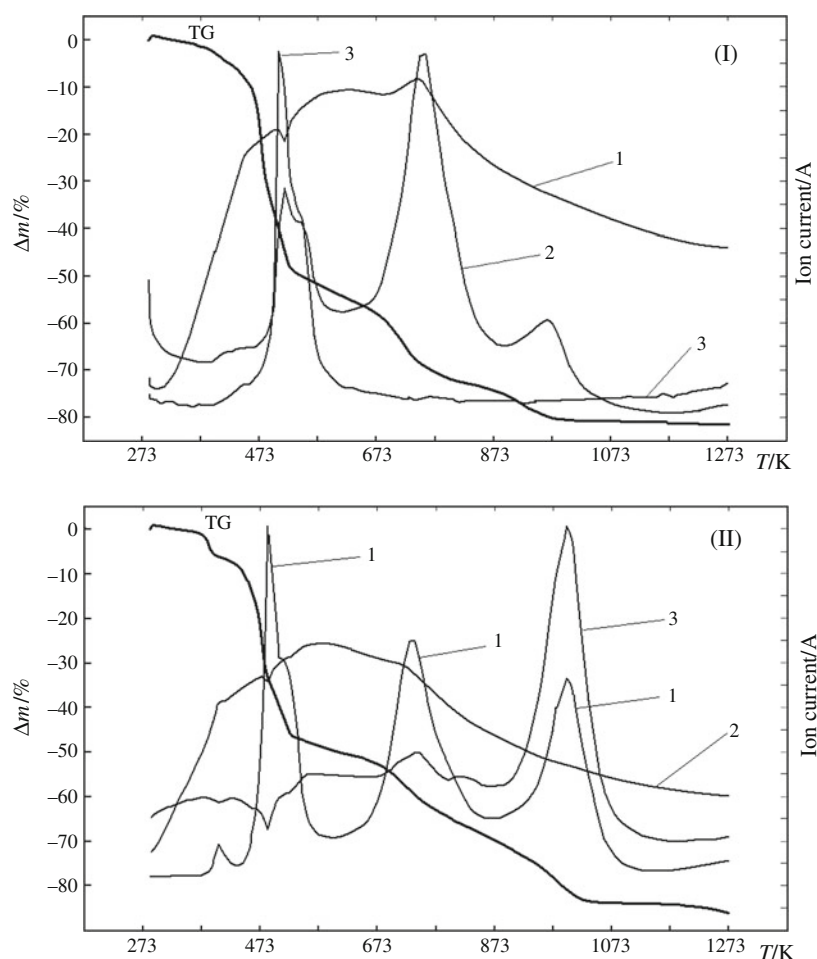


Fig. 4 TG curve for Pr(III) (I) and Sm(III) (II) complexes and ion current detected by the MS for mass fragments in air; (I) m/z 1–18; 2–43; 3–72 with sensitivity of ion current: E-9, E-11, E-12, respectively, mass sample 4.64 mg; (II) m/z 1–12; 2–18; 3–30 with sensitivity of ion current: E-10, E-8, E-9, respectively, mass sample 4.82 mg



oxidation of organic ligands and combustion of remaining organic fragments (Fig. 2).

The complex of $\text{Pr}(4\text{-bpy})_{1.5}(\text{CCl}_3\text{COO})_3 \cdot \text{H}_2\text{O}$ loses water molecule in first stage (333–391 K). The dehydration process is accompanied by small endothermic effects (388 K). The anhydrous compound is stable up to 391 K. Next, total decomposition of trichloroacetates takes place and intermediate specie $\text{Pr}(4\text{-bpy})_{1.5}\text{Cl}_3$ (391–513 K) is formed. DTA curve presents exo peak at 503 K. On temperature elevation (513–1053 K) $\text{Pr}(4\text{-bpy})_{1.5}\text{Cl}_3$ directly decomposes to Pr_6O_{11} .

The dehydration process of complex $\text{Sm}(4\text{-bpy})_{1.5}(\text{CCl}_3\text{COO})_3 \cdot \text{H}_2\text{O}$ is connected with partial decomposition of trichloroacetate ligands (333–418 K), which are demonstrated by endothermic peak on DTA curve (378 K). Probably $\text{Sm}(4\text{-bpy})_{1.5}(\text{CCl}_3\text{COO})_{2.25}\text{Cl}_{0.75}$ is formed. When the temperature raises it converts to $\text{Sm}(4\text{-bpy})_{1.5}\text{Cl}_3$ (exo peak at 453 K). Next the 4-bpy is lost (probably via intermediate species $\text{Sm}(4\text{-bpy})_{1.5-m}\text{Cl}_3$), together with anions (2Cl^-), and SmOCl occurs. A constant mass level for pure Sm_2O_3 appears above 1053 K.

The pyrolysis of Eu(III) compound is multistage. In the ranges of temperature: 333–408, 408–468, and 468–893 K

intermediate species $\text{Eu}(4\text{-bpy})_{1.5}(\text{CCl}_3\text{COO})_{1.75}\text{Cl}_{1.25}$, $\text{Eu}(4\text{-bpy})_{1.5}\text{Cl}_3$ and EuOCl (probably via $\text{Eu}(4\text{-bpy})_{1.5-m}\text{Cl}_3$) are created, respectively. On the DTA curve endo- and exothermic peaks exist. Formation of pure Eu_2O_3 begins above 893 K.

Thermolysis of $\text{Gd}(4\text{-bpy})_{1.5}(\text{CCl}_3\text{COO})_3 \cdot 3\text{H}_2\text{O}$ complex starts with dehydration and partial decomposition of trichloroacetates $\text{Gd}(4\text{-bpy})_{1.5}(\text{CCl}_3\text{COO})_2\text{Cl}$ (333–413 K). It converts to $\text{Gd}(4\text{-bpy})_{1.5}\text{Cl}_3$. These processes are accompanied with endo and exo effects at 368 and 463 K, respectively. When the temperature rises, further decomposition of organic ligands is similar to Eu(III) compound. In the range 763–1043 K GdOCl is formed. On DTA curve exo peaks at 813 and 1023 K appear. Above 1123 K pure Gd_2O_3 exists.

The $\text{Tb}(4\text{-bpy})_{1.5}(\text{CCl}_3\text{COO})_3 \cdot 3\text{H}_2\text{O}$ complex decomposes in the temperature range 333–403 K. Dehydration is connected with partial pyrolysis of trichloroacetate ligands and forms intermediate $\text{Tb}(4\text{-bpy})_{1.5}(\text{CCl}_3\text{COO})_2\text{Cl}$. This process is characterized by endo effect at 353 K. Next, the step-wise decomposition of organic ligands takes place (453 and 723 K exo peaks). The final solid product of decomposition is Tb_4O_7 (via TbOCl).

Mass spectrometry

A coupled TG-MS system has been used to study volatile species and fragments evolved during the dynamic thermal decomposition of $\text{Ln}(4\text{-bpy})_{1.5}(\text{CCl}_3\text{COO})_3 \cdot n\text{H}_2\text{O}$ (where Ln(III) = Pr, Sm) in air atmosphere. MS data of Pr(III) and Sm(III) complexes are very similar. They detected several ions signal intensities. Figure 3 presents some profiles of ion current for m/z values detected in the mass spectrometer versus time for these complexes in air. Generally, many signals are observed in the range 373–593 K. The m/z values are given for ^1H , ^{12}C , ^{14}N , ^{16}O (additionally ^{13}C and ^{18}O). The profiles observed for OH^+ and H_2O^+ are ample. They show the mixture a sufficient dehydration by the release of hydrogen in form of crystalline (or coordination) of H_2O in first step and the large amount attributed to oxidation of the organic matter above. In gaseous pyrolysis products dominate ion C^+ and CO_2^+ ($m/z=12, 44$) with centers at 448, 576, 756, 971 K (Pr(III)) and 402, 486, 733, 998 K (Sm(III)). The first maxima of these species coincide with beginning of trichloroacetate ligands decomposition. Further peaks are connected with the total decomposition of ligands and the burning of organic residues. Probably maximum rate of forming of NO^+ (or CH_2O^+ $m/z = 30$) at 649 K for Pr(III) and 651 K for Sm(III) complexes (traces of N_2O_3 with $m/z = 76$ at 590 K for Pr(III) and Sm(III)) are observed. The mass spectrometer was also monitoring of species containing halogens: Cl^+ , HCl^+ , CCl^+ , CH_2Cl^+ , CH_3Cl^+ , CH_2Cl_2^+ ($m/z = 35, 36, 47, 49, 50, 84$). Additionally, ion currents with $m/z = 27, 29, 43, 70, 72$ and 74 (HCN^+ , CHO^+ , CHNO , $^{35}\text{Cl}_2^+$, $^{35}\text{Cl}^{37}\text{Cl}^+$, $^{37}\text{Cl}_2^+$) were monitored. The ion currents for different fragments are illustrated together with the corresponding TG (Fig. 4).

Conclusions

Now, the new fine-crystalline compounds with stoichiometry: $\text{Ln}(4\text{-bpy})_{1.5}(\text{CCl}_3\text{COO})_3 \cdot n\text{H}_2\text{O}$ (where Ln(III) = Pr, Sm, Eu, Gd, Tb; $n = 1$ for Pr, Sm, Eu and $n = 3$ for Gd, Tb) were isolated. The IR spectra give us the information about different coordination of organic ligands. Resting on $\Delta\nu$, we can see, that Pr(III), Sm(III) and Eu(III) complexes possess bidentate chelating $-\text{COO}$ groups. In the case of Gd(III) and Tb(III) probably non-completely equivalent bands between these ions and carboxylate groups are formed. Conductivity data show, that trichloroacetate ligands are inside coordination sphere. All obtained complexes are stable at room temperature. During heating they decompose progressively. Only a monohydrated Pr(III) compound loses water molecule over the range 333–391 K, and next decomposes via $\text{Pr}(4\text{-bpy})_{1.5}\text{Cl}_3$ to Pr_6O_{11} . For the

other complexes dehydration is united with partial decomposition of trichloroacetates. When the temperature rises total decomposition of organic ligands takes place. The final solid products are the oxides: Ln_2O_3 (Ln(III) = Sm, Eu, Gd) and Tb_4O_7 .

Open Access This article is distributed under the terms of the Creative Commons Attribution Noncommercial License which permits any noncommercial use, distribution, and reproduction in any medium, provided the original author(s) and source are credited.

References

1. Radwańska-Doczekalska J, Czakis-Sulikowska D, Markiewicz M. Synthesis, structural characterisation and thermal decomposition studies of some 2,4'-bipyridyl complexes with cobalt(II), nickel(II) and copper(II). *J Therm Anal Calorim.* 1997;48: 865–75.
2. Czakis-Sulikowska D, Czyłkowska A, Radwańska-Doczekalska J. Synthesis and thermal properties of 4,4'-bipyridine adducts of Mn(II), Co(II), Ni(II) and Cu(II) monochloroacetate. *J Therm Anal Calorim.* 2001;63:387–95. doi:10.1023/A:1010188325149.
3. Czakis-Sulikowska D, Czyłkowska A, Malinowska A. Some dn metal complexes with 4,4'-bipyridine and trichloroacetates. Preparation, characterization and thermal properties. *J Therm Anal Calorim.* 2001;65:505–13. doi:10.1023/A:1012493406026.
4. Czakis-Sulikowska D, Czyłkowska A, Malinowska A. Thermal and other properties of new 4,4'-bipyridine-trichloroacetato complexes of Mn(II), Ni(II) and Zn(II) *ibid.* *J Therm Anal Calorim.* 2001;67:667. doi:10.1023/A:1014365007321.
5. Czakis-Sulikowska D, Czyłkowska A. Complexes of Mn(II), Co(II), Ni(II) and Cu(II) with 4,4'-bipyridine and dichloroacetates. *J Therm Anal Calorim.* 2003;71:395–405. doi:10.1023/A:1022 879120867.
6. Czakis-Sulikowska D, Czyłkowska A. Thermal and other properties of complexes of Mn(II), Co(II) and Ni(II) with 2,2'-bipyridine and trichloroacetates *ibid.* *J Therm Anal Calorim.* 2003;74:349–60. doi:10.1023/A:1026371029185.
7. Czakis-Sulikowska D, Czyłkowska A. Synthesis, thermal and other studies of 2,4'-bipyridine-dichloroacetato complexes of Mn(II), Co(II), Ni(II) and Cu(II) *ibid.* *J Therm Anal Calorim.* 2004;76:543–55. doi:10.1023/B:JTAN.0000028033.91256.c6.
8. Blower PJ. Inorganic pharmaceuticals. *Annu Rep Prog Chem A.* 2000;96:645–62. doi:10.1039/B003162N.
9. Sherry AD. MR imaging and spectroscopy applications of lanthanide complexes with macrocyclic phosphonate and phosphonate ester ligands. *J Alloy Comp.* 1997;249:153–7. doi:10.1016/S0925-8388(96)02518-2.
10. Woods M, Kavacs Z, Sherry AD. Targeted complexes of lanthanide(III) ions as therapeutic and diagnostic pharmaceuticals. *J Supramol Chem.* 2002;2:1–15. doi:10.1016/S1472-7862(02) 00072-2.
11. Chang WB, Zhang BL, Li LZ, Ci YX. Double-label simultaneous time-resolved fluoroimmunoassay of phenytoin and phenobarbital. *Microchem J.* 1997;55:287–95. doi:10.1006/mchj.1996.1305.
12. Ferri D, Forni L. Methane combustion on some perovskite-like mixed oxides. *Appl Catal B Environ.* 1998;16:119–26. doi:10.1016/S0926-3373(97)00065-9.
13. Parac-Vogt TN, Binnemans K. Lanthanide(III) nosylates as new nitration catalysts. *Tetrahedron Lett.* 2004;45:3137–9. doi:10.1016/j.tetlet.2004.02.084.
14. Oczko G, Starynowicz P. Comparison of optical properties and crystal structures of the praseodymium and europium

- chloroderivatives of acetates. *J Mol Struct.* 2005;740:237–48. doi:10.1016/j.molstruc.2004.12.018.
15. Oczko G, Legendziewicz J, Mroziński J, Meyer G. Comparative spectroscopic and magnetic studies of two types of Ln and Ln:Cu trichloroacetates. *J Alloys Comp.* 1998;219:275–7.
 16. Legendziewicz J, Borzechowska M, Oczko G, Mroziński J. Polymeric polynuclear systems of Pr, Yb and Pr:Cu trichloroacetates; their spectroscopy and magnetism. *Spectrochimica Acta A.* 1998;54:2197–205. doi:10.1016/S1386-1425(98)00138-3.
 17. Voronkova VK, Galeev RT, Legendziewicz J, Oczko G (2000) EPR spectra of alternating chains in $(\text{Nd}_2(\text{CCl}_3\text{COO})_6(\text{H}_2\text{O})_3)_n \cdot n\text{H}_2\text{O}$. XIIIth Winter School on Coordination Chemistry, Karpacz, 4–8 December, 89.
 18. Voronkova VK, Yablokov V, Oczko G (1996) Polynuclear complexes of lanthanides with trichloroacetate ligands: syntheses, structures and EPR studies of $\text{Nd}(\text{CCl}_3\text{COO})_3 \cdot 2\text{H}_2\text{O}$, $(\text{Nd}, \text{Cu})(\text{CCl}_3\text{COO})_8 \cdot 6\text{H}_2\text{O}$ and $(\text{Nd}, \text{La})(\text{CCl}_3\text{COO})_3 \cdot 2\text{H}_2\text{O}$. XIIIth Summer School on Coordination Chemistry, Polanica Zdrój, 2–8 June, 177.
 19. Barja B, Baggio R, Garland MT, Aramendio PF, Pena O, Perec M. Crystal structures and luminescent properties of terbium(III) carboxylates. *Inorg Chim Acta.* 2003;346:187–96. doi:10.1016/S0020-1693(02)01429-9.
 20. Rohde A, Urland W. Synthesis and crystal structures of $\text{Ln}(\text{ClF}_2\text{CCOO})_3(\text{H}_2\text{O})_3$ (Ln = Gd, Dy, Ho, Er) and magnetic behaviour of $\text{Gd}(\text{ClF}_2\text{CCOO})_3(\text{H}_2\text{O})_3$. *Z Anorg Allg Chem.* 2004;630:2434–7. doi:10.1002/zaac.200400173.
 21. Oczko G. Spectroscopic properties of neodymium monochloroacetate single crystal as an example of complex containing Nd(III) in three different symmetry Sites. *J Alloys Compd.* 2000;300:414–20. doi:10.1016/S0925-8388(99)00754-9.
 22. Imai T, Shimoi M, Ouchi Z. The crystal and molecular structure of the hydrated light lanthanoid(III) chloroacetates, $[\{\text{M}(\text{ClCH}_2\text{CO}_2)_3\}_3(\text{H}_2\text{O})_5]_n$, (M = La, Pr, Nd and Eu). *Bull Chem Soc Japan.* 1987;60:159–69. doi:10.1246/bcsj.60.159.
 23. Rohde A, Urland W. Catena-poly[[2, 200-bipyridine- η^2 N, N00]-neodymium(III)]-1-dichloroacetato-1 η^2 O:O00:2 η^2 Odi-1-dichloroacetato- η^4 O:O00]. *Acta Crystallogr Sec E.* 2006;62(7):m1618–9. doi:10.1107/S1600536806022872.
 24. Rohde A, Urland W. Catena-Poly[[2, 200-bipyridine- η^2 N, N']-praseodymium(III)]-1-dichloroacetato-1 η^2 O:O':2O-di-1-dichloroacetato-4O:O']. *Acta Crystallogr Sec E.* 2006;62(11):m2843–5. doi:10.1107/S160053680603995X.
 25. John D, Urland W. Synthesis, crystal structure, and magnetic behaviour of $[\text{Gd}_2(\text{ClF}_2\text{CCOO})_6(\text{H}_2\text{O})_2(\text{bipy})_2]_2 \cdot \text{C}_2\text{H}_5\text{OH}$. *Z Anorg Allg Chem.* 2006;632(10):1768–70. doi:10.1002/zaac.200500400.
 26. John D, Urland W. Crystal Structure and magnetic behaviour of the new gadolinium complex compound $\text{Gd}_2(\text{ClF}_2\text{CCOO})_6(\text{bipy})_2$. *Eur J Inorg Chem.* 2005;22:4486–9. doi:10.1002/ejic.200500734.
 27. Rohde A, John D, Urland W. Crystal structures of $\text{Gd}_2(\text{Cl}_3\text{CCOO})_6(\text{bipy})_2(\text{H}_2\text{O})_2 \cdot 4\text{-bipy}$, $\text{Pr}(\text{Cl}_3\text{CCOO})_3(\text{bipy})_2$, $\text{Nd}(\text{Cl}_3\text{CCOO})_3(\text{bipy})_2$ and $\text{Er}(\text{Cl}_3\text{CCOO})_3(\text{bipy})_2(\text{H}_2\text{O})$. *Z Kristal.* 2005;220(2):177–82. doi:10.1524/zkri.220.2.177.59141.
 28. Spacu F, Antonescu E. Complexes of lanthanide haloacetates with 1, 10-phenanthroline and 2,2'-bipyridine. *Rev Roumaine Chim.* 1969;14:201–7.
 29. Hart FA, Laming J. Lanthanide complexes-III: complexes of 2,2'-dipyridyl with lanthanide chlorides, thiocyanates, acetates and nitrates. *J Nucl Chem.* 1965;27:1825–9. doi:10.1016/0022-1902(65)80326-8.
 30. Kokonov JV, Segal EJ. Thermal decomposition of complexes of neodymium and erbium with 1, 10-phenanthroline and 2,2'-bipyridyl. *Rev Roumaine Chim.* 1971;16:1647–50.
 31. Batten A, Robson R. Interpenetrating nets: ordered, periodic entanglement. *Angew Chem Int Ed.* 1998;37:1461–94. doi:10.1002/(SICI)1521-3773(19980619).
 32. Janiak C. Functional organic analogues of zeolites based on metal–organic coordination frameworks. *Angew Chem Int Ed Engl.* 1997;36:1431–4. doi:10.1002/anie.199714311.
 33. Tao J, Tong ML, Chen XM (2000) Hydrothermal synthesis and crystal structures of three-dimensional co-ordination frameworks constructed with mixed terephthalate (tp) and 4,4'-bipyridine (4,4'-bipy) ligands: $[\text{M}(\text{tp})(4,4'\text{-bipy})]$ (M = Co^{II} , Cd^{II} or Zn^{II}). *J Chem Soc Dalton Trans.* 3669–3674.
 34. Zaworotko MJ. Superstructural diversity in two dimensions: crystal engineering of laminated solids. *Chem Commun.* 2001;1:1–9.
 35. Czylkowska A, Kruszyński R, Czakis-Sulikowska D, Markiewicz M. Coordination polymer of lanthanum: synthesis, properties and crystal structure of $[\text{La}(4,4'\text{-bipyridine})(\text{CCl}_2\text{HCOO})_3(\text{H}_2\text{O})]_n$. *J Coord Chem.* 2007;60:2659–69. doi:10.1080/00958970701299550.
 36. Sain S, Maji TK, Mostafa G, Lu TH, Chudhuri VR. Two new supramolecular malonato complexes of manganese(II): synthesis, crystal structure and magnetic property. *Inorg Chim Acta.* 2003;351:12–20.
 37. Li JM, Zhang YG, Chen JH, Wang QM, Wu XT. Microporous networks co-assembled by both rigid and flexible building blocks. *Polyhedron.* 2000;19:1117–21. doi:10.1016/S0277-5387(00)00361-2.
 38. Tao I, Yin X, Huang R, Zhang L. Hydrothermal synthesis of a novel microporous framework sustained by polycatenated $[\text{Cu}_2(\text{ip})(4,4'\text{-bipyridine})]_n$ (ip = isophthalate) ladders. *Inorg Chem Commun.* 2001;5:1000–2. doi:10.1016/S1387-7003(02)00624-X.
 39. Carballo R, Castiñeiras A, Covelo B, Vázquez-Lopez EM. Coordination polymers of copper(II) based on mixed N- and O-donor ligands: the crystal structures of $[\text{CuL}_2(4,4'\text{-bipy})]_n$ (L = lactate or 2-methylactate). *Polyhedron.* 2001;20:899–904. doi:10.1016/S0277-5387(01)00749-5.
 40. Czakis-Sulikowska D, Czylkowska A, Markiewicz M. Synthesis, characterization and thermal decomposition of yttrium and light lanthanides with 4,4'-bipyridine and dichloroacetates. *Polish J Chem.* 2007;81:1267–75.
 41. Kruszyński R, Czylkowska A, Czakis-Sulikowska D. A novel carboxylic coordination polymer of samarium(III): $[\text{Sm}(\text{H}_2\text{O})(4,4'\text{-bipyridine})(\text{CCl}_2\text{HCOO})_3]_n$. *J Coord Chem.* 2006;59:681–90. doi:10.1080/00958970500345356.
 42. Czakis-Sulikowska D, Czylkowska A, Markiewicz M, Frajta M. Synthesis and properties of complexes of Gd(III), Tb(III), Ho(III) and Tm(III) with 4,4'-bipyridine and dichloroacetates. *Polish J Chem.* 2009;83:1893–901.
 43. Czylkowska A, Markiewicz M. Coordination behaviour and thermolysis of some rare-earth complexes with 4,4'-bipyridine and di- or trichloroacetates. *J Therm Anal Calorim.* 2010;100:717–23. doi:10.1007/s10973-009-0182-5.
 44. Czylkowska A, Czakis-Sulikowska D, Kruszyński R, Markiewicz M. Synthesis, crystal structure and other properties of the complexes of Er(III), Yb(III) and Lu(III) with 4,4'-bipyridine and dichloroacetates. *Struct Chem.* 2009;21:415–23. doi:10.1007/s11224-009-9545-6.
 45. Powder diffraction file, PDF-2, release 2004. The international centre for diffraction data (ICDD) 12 Campus Boulevard, Newton Square, PA, USA.
 46. Geary WI. The use of conductivity measurements in organic solvents for the characterisation of coordination compounds. *Coord Chem Rev.* 1971;7:81–122. doi:10.1016/S0010-8545(00)80009-0.
 47. Pearce CK, Grosse DW, Hessel W. Effect of molecular structure on infrared spectra of six isomers of bipyridine. *Chem Eng Data.* 1970;15:567–70. doi:10.1021/jc60047a042.
 48. Deacon GB, Philips RI. Relationships between the carbon-oxygen stretching frequencies of carboxylato complexes and the type of carboxylate coordination. *Coord Chem Rev.* 1980;33:227–50. doi:10.1016/S0010-8545(00)80455-5.

49. Nakamoto K. Infrared and Raman spectra of inorganic and coordination compounds. New York: Wiley; 2009.
50. Manhas BS, Trikha AK. Relationships between the direction of shifts in the carbon-oxygen stretching frequencies of carboxylato complexes and the type of carboxylate coordination. *Indian J Chem.* 1982;59:315–9.
51. Brzyska W, Ożga W. Spectral, magnetic and thermal investigations of some *d*-electron element 3-methoxy-4-methylbenzoates. *J Therm Anal Calorim.* 2006;84:385–9. doi:[10.1007/s10973-005-6855-9](https://doi.org/10.1007/s10973-005-6855-9).
52. Zelenak V, Vargova Z, Gyoryova K. Correlation of infrared spectra of zinc(II) carboxylates with their structures. *Spectrochimica Acta, A.* 2007;66:262–72. doi:[10.1016/j.saa.2006.02.050](https://doi.org/10.1016/j.saa.2006.02.050).
53. Brzyska W, Dębska E, Szczotka M. New complexes of rare earth elements with methylsuccinic acid. *Polish J Chem.* 2001;75:1393–9.
54. Brzyska W, Ożga W. Preparation, properties and thermal decomposition of silver(I) complexes with pyridinedicarboxylic acids. *Polish J Chem.* 1997;71:436–40.